Synthesis and Properties of Silica–Polyimide Hybrid Films Derived from Colloidal Silica Particles and Polyamic Acid

Zhenping Shang,[1] Changli Lü,[2] Xiaodan Lü,[2] Lianxun Gao[1]

[1]*State Key Laboratory of Polymer Physics and Chemistry, Changchun Institute of Applied Chemistry, Graduate School of Chinese Academy of Science, Chinese Academy of Sciences, Changchun 130022, People's Republic of China*
[2]*Institute of Chemistry, Northeast Normal University, Changchun 130024, People's Republic of China*

Received 25 May 2006; accepted 5 October 2006
DOI 10.1002/app.27657
Published online 2 June 2008 in Wiley InterScience (www.interscience.wiley.com).

ABSTRACT: A series of SiO_2/polyimide hybrid films with different contents and sizes of SiO_2 particles were prepared by blending polyamic acid (PAA) and SiO_2 nanoparticles obtained from Stöber method, followed by a step thermal imidization process. The size and content effect of SiO_2 particles on the mechanical and thermal properties was studied. It was found that as the silica particles were introduced into polyimide matrix, T_gs of hybrid films increased on the whole and there was a maximum value of T_g for the hybrid film with 10-nm SiO_2 particles. TGA indicated that the thermal stability for hybrid films decreased with the increasing content and size of SiO_2 particles. Dynamic mechanical thermal analysis (DMTA) indicated that the modulus of hybrid films increased, while the tensile strength and elongation at break decreased as the size of SiO_2 particles increases from 10 to 25 nm and to 65 nm. All polyimide hybrid films were amorphous according to X-ray determination. © 2008 Wiley Periodicals, Inc. J Appl Polym Sci 109: 3477–3483, 2008

Key words: polyimide; SiO_2 colloidal particles; hybrid films; properties

INTRODUCTION

Inorganic/organic hybrid materials have attracted considerable attention because these hybrids combine the advantages of organic polymer (flexibility, good processability) and inorganic materials (high thermal stability and chemical resistance).[1–3] Recently, high-performance polyimide hybrids have been widely studied by incorporating inorganic materials into polyimide matrix.[4,5] In particular, the polyimide hybrid materials with dimension in the nanometer size have been largely focused on, because they exhibited better thermal, mechanical, gas separation, and dielectric properties. For example, many polyimide-based nanocomposites, including TiO_2/PI,[6,7] silica/PI,[5,8–10] ZnO/PI,[11] Al_2O_3/PI,[12] $BaTiO_3$/PI,[13] and polyhedral oligomeric silsesquioxanes/PI,[14–16] have been prepared. At present, the most studies are focused on the silica/polyimide hybrids. The general approach for preparing silica/polyimide hybrids is the sol–gel technique, which includes the hydrolysis of alkoxysilane and polycondensation of the hydrolysis products.[5] This method allows one to control the microstructure and interfacial properties of the composites.

Another method for preparing hybrid materials can be carried out by introducing colloidal silica particles into PI matrices via blending process. This method provides full synthetic control over the particle size and size distribution as well as the surface properties of nanoparticles. Here, Stöber method can provide a facile route for synthesizing silica nanoparticles with different sizes.[17] However, the preparation of PI-based hybrid materials with different SiO_2 sizes and the effect of SiO_2 size on the properties of hybrid materials have never been studied. In this article, we prepared a series of SiO_2/polyimide hybrid films with different contents and size of SiO_2 particles by blending polyimide and colloidal silica nanoparticles obtained from Stöber method. The microstructure of hybrids and the influence of particle size and content on the mechanical and thermal properties were studied in detail.

EXPERIMENTAL

Materials

Pyromellitic dianhydride (PMDA, 99%) and 4,4′-oxydianiline (ODA, 99%) were purchased from Shanghai Chemical Reagents Company, and were purified by sublimation under vacuum. *N*,*N*-dimethylaceta-

Correspondence to: L. Gao (lxgao@ciac.jl.cn).
Contract grant sponsor: National Natural Science Foundation of China; contract grant number: 50333030.

TABLE I
Recipes for Synthesis of Colloidal Silica Particles with Different Sizes

Particle sizes (nm)	Recipes (mL)		
	TEOS	$NH_3 \cdot H_2O$	EtOH
10	8	5	190
25	8	7	190
65	8	10	190

mide (DMAc, 99.5%) was purified by distillation over phosphorus pentoxide and stored over 4 Å molecular sieves. Tetraethoxysilane (TEOS, SiO_2 content 28.5 wt %), absolute ethanol (99.7%), and ammonium hydroxide (25–28% ammonia content) were of analytical grade and used as received.

Synthesis of PAA

PAA was synthesized from PMDA and ODA by one-step process in DMAc.[18] ODA (4.00 g, 20 mmol) was dissolved in dry DMAc with stirring, and then PMDA (4.36 g, 20 mmol) was added in ODA solution at room temperature. After the mixture was stirred for 24 h, a 10 wt % solution of PAA in DMAc was obtained.

Synthesis of colloidal silica particles

Colloidal silica nanoparticles with mean size of 10, 25, and 65 nm were synthesized in ethanol at an ambient temperature via Stöber method,[17] respectively. The recipes for preparing colloidal silica particles with different sizes are shown in Table I. The representative sample for the synthesis of colloidal silica with 10 nm in mean diameter is as follows: 5-mL $NH_3 \cdot H_2O$ and 150-mL ethanol (EtOH) were added into 250-mL three-necked round bottom flask, then 8-mL TEOS in 40-mL ethanol were dropped within 30 min, and the reaction was allowed to stir for 24 h at room temperature. The resulted colloidal silica sol was condensed under vacuum at 30°C to remove partial ethanol to form about 5–10 wt % of colloidal silica sol.

Preparation of PI/SiO_2 hybrid films

The colloidal silica particles with different sizes were mixed with PAA solution in the desired weight ratio. Most of the ethanol was removed from mixture at room temperature to obtain a viscous mixture solution with about 5 wt % solid content in DMAc. The composite films were prepared by casting the homogeneous viscous solution onto glass plates on a hot plate at 60°C. The films were cured on a hot plate at 60°C for 12 h, and then a step thermal imidization process (0.5 h each at 100, 150, 200, 250°C, finally at 300°C for 2 h) was carried out.

Characterization

FTIR spectra were recorded on a Nicolet AVATAR360 FTIR spectrometer. Thermogravimetric analyses (TGA) were obtained at a heating rate of 20°C/min in nitrogen with a Perkin-Elemer TGA-2 thermogravimetric analyzer. The glass transition temperature (T_g) of hybrid films was measured on a dynamic mechanical thermal analyzer (DMTA) using film samples (length: 10 mm). The run conditions were conducted at a frequency of 1 Hz and a heating rate of 3°C/min in a tensile mode. The tensile measurements were carried out on an Instron model 1122 at a testing rate of 5 mm/min at room temperature according to the standard GB/T 1040-1992. The wide-angle X-ray diffraction (WAXD) measurements were undertaken on a Rigaku max 2500 V PC X-ray diffractometer with Cu Kα radiation (40 kV, 200 mA) with a scanning rate of 2°/min from 5 to 50°. The morphologies of fractured surfaces of hybrid films were studied with an XL-30 ESEM FEG Scanning Electron Microscope (FEI Company, Hillsboro, OR). Transmission electron microscopy (TEM) was carried out using a JEOL-2021 microscope. Hybrid samples with a thickness of about 70–100 nm on copper grid for TEM were prepared by ultramicrotoming. Water absorption experiments were performed on the four pieces of film samples with mass ranging from 100 to 150 mg, and the films were heated at 180°C for 1 h to remove the water to get the initial weight of the film before soaking in water. The above treated film samples were immersed in deionized water at 25°C, and water absorption equilibrium was considered to attain after 10 days. The weight gains were measured as percent of the water absorption.

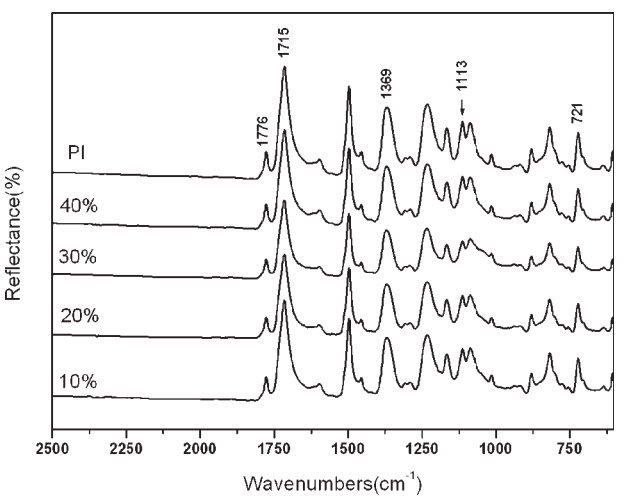

Figure 1 FTIR spectra of PI/10-nm SiO_2 hybrid films with different SiO_2 contents.

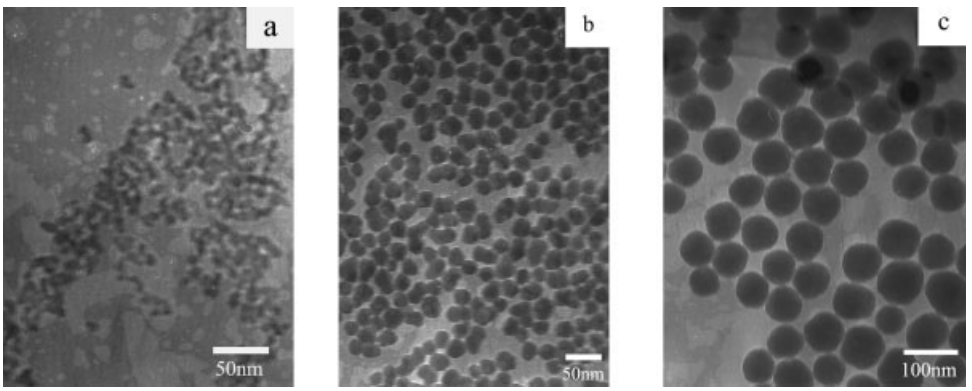

Figure 2 TEM images of the colloidal SiO_2 particles: (a) 10 nm, (b) 25 nm, and (c) 65 nm.

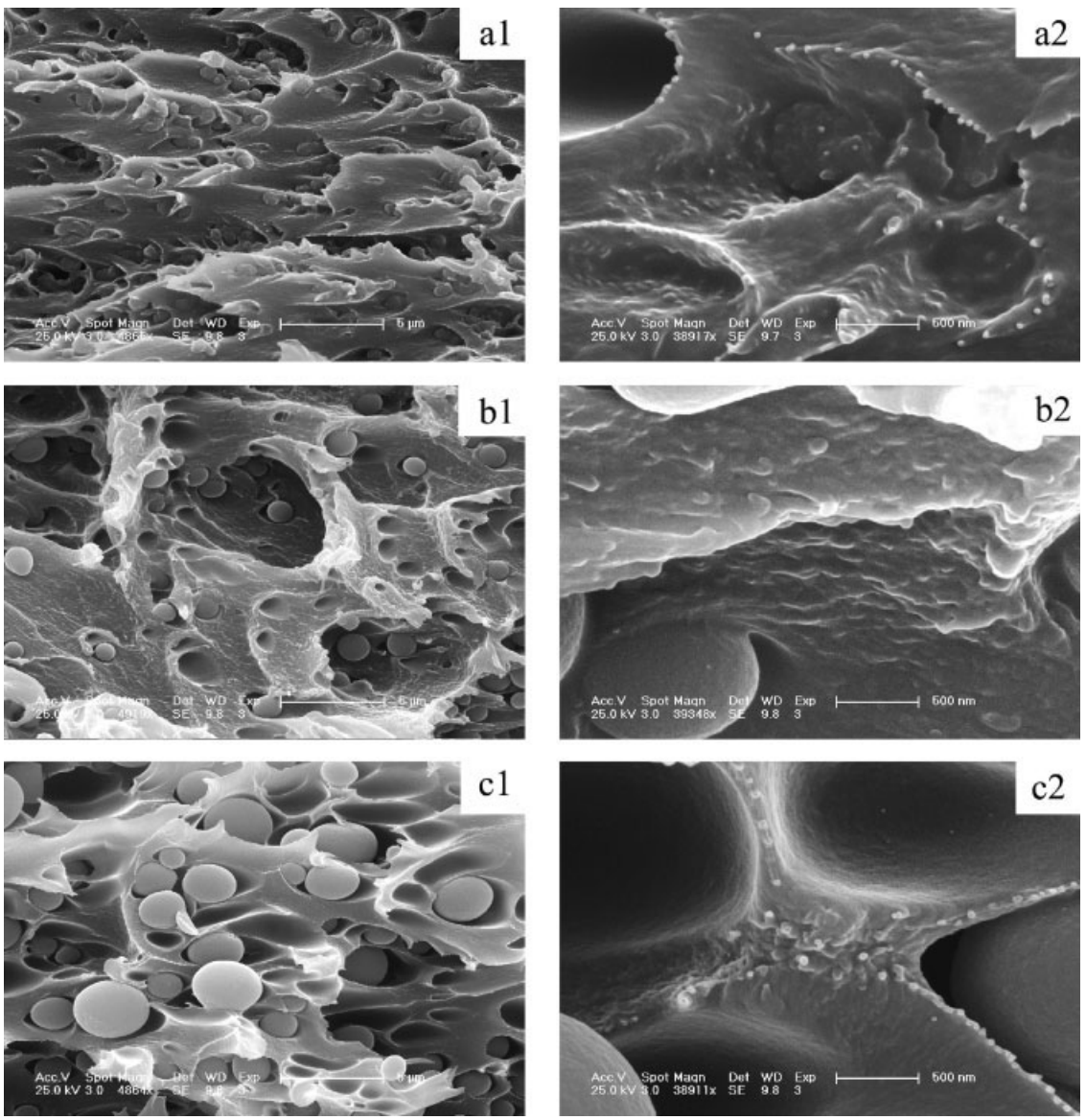

Figure 3 SEM images of the fracture surface of PI/10 wt % SiO_2 hybrids with different sizes of SiO_2 (a1, a2) 10 nm, (b1, b2) 25 nm, (c1, c2) 65 nm (image 2 is the magnification image).

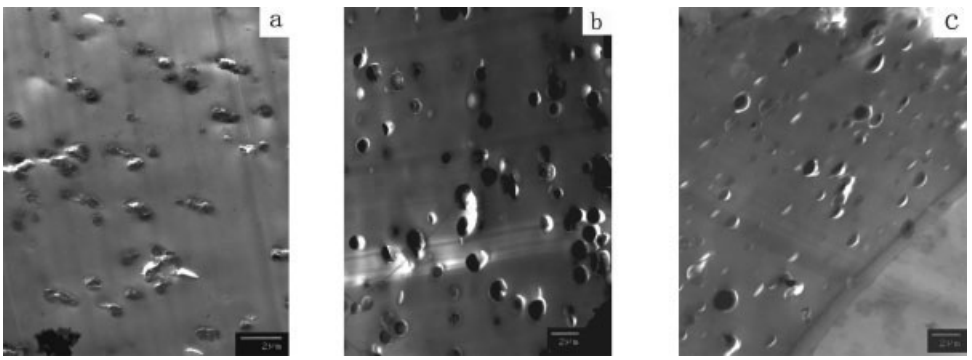

Figure 4 TEM images of the PI/10 wt % SiO_2 hybrids with different sizes of SiO_2: (a) 10 nm, (b) 25 nm, and (c) 65 nm.

RESULTS AND DISCUSSION

FTIR analysis

Figure 1 shows the FTIR spectra of the PI/10-nm SiO_2 hybrid films. It can be seen that the peaks near at 1776 (C=O symmetric stretching), 1715 (C=O asymmetric stretching), 1369 (C—N stretching), 1113, and 721 cm^{-1} attributed to the characteristic absorptions of imide groups.[18] The absorption peaks of polyamic acid (PAA) at 1650 cm^{-1} disappears, indicating that the imidization reaction is complete.[19,20] The absorption band of Si—O—Si bond at 1000–1100 cm^{-1} and the band of imide groups overlap, although the differences could not be clearly observed. However, the absorption bands of Si—O—Si in PI/SiO_2 hybrids become broader and their intensity also gradually increase with increasing SiO_2 particle content, compared with the intensity of the characteristic peaks of imide groups. This suggests that an increasing amount of SiO_2 was successfully introduced into the polymer matrix.

Microstructure of hybrid films

The original colloidal SiO_2 particles for preparing PI-based hybrids have three different sizes of 10, 25, and 65 nm in average diameter. Figure 2 shows the images of the original colloidal SiO_2 particles. SEM images of the 10 wt % SiO_2/PI hybrid films with different SiO_2 sizes are shown in Figure 3. It can be seen that there are two types of SiO_2 spheres with large and small size for the different hybrids. Compared with original SiO_2 particles before blending, the partial SiO_2 particles aggregated to form large silica spheres (several hundred nanometer to two micrometer) with primary particles inside, and the size of large SiO_2 also increases with increasing size of original silica particles. It is possible that the surface of SiO_2 modified without organic molecules, results in the aggregation of original colloidal SiO_2 and formation of large SiO_2 spheres. In addition, many small primary SiO_2 particles exist in the hybrid films and they are imbedded in polymer matrices, which favor for the improvement of thermal

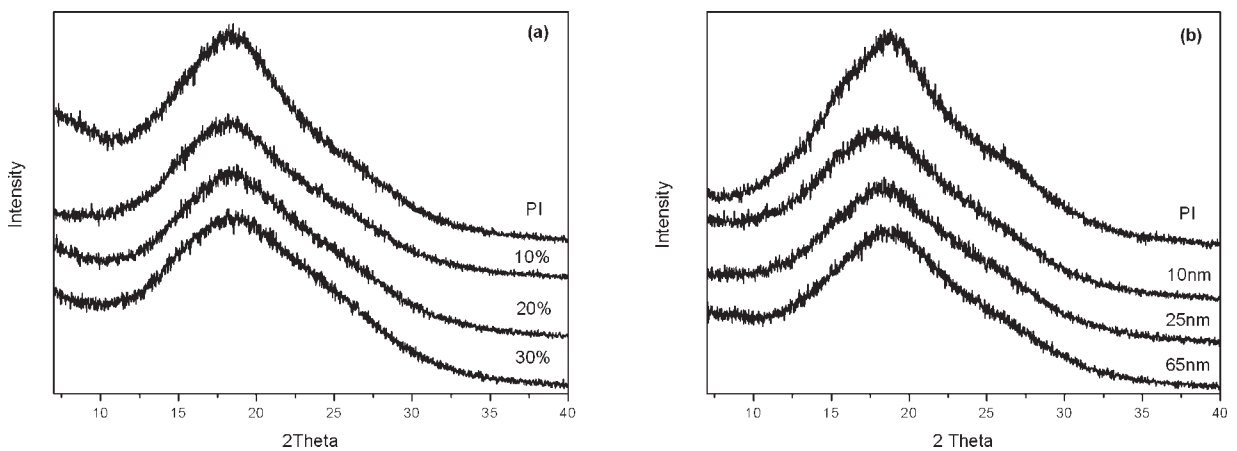

Figure 5 X-ray diffraction patterns of (a) PI/10-nm SiO_2 hybrids with different SiO_2 contents and (b) PI/10 wt % SiO_2 hybrids with different SiO_2 sizes.

TABLE II
Properties of PI/10-nm SiO_2 Hybrid Films

Samples	Modulus (MPa)	Tensile strength (MPa)	Elongation (%)	Density (g/cm^3)	R_{wa} (wt %)[a]	T_d (°C)[b]	T_g (°C)[c]
PI	1,654	219	83	1.353	3.08	570	389.2
PI-5-SiO_2	1,869	195	79	1.398	3.26	565	400.3
PI-10-SiO_2	1,887	163	65	1.413	3.59	566	399.6
PI-15-SiO_2	1,950	160	60	1.419	4.08	561	398.1
PI-20-SiO_2	2,110	149	41	1.422	4.43	557	410.6
PI-30-SiO_2	2,180	145	38	1.519	5.09	535	400.0
PI-40-SiO_2	2,540	123	36	1.543	6.29	499	398.3

[a] Water absorption of hybrid films.
[b] 5 wt % decomposition temperature.
[c] Glass transition temperature of hybrid films obtained by DMTA.

and mechanical properties. Many holes were also observed in hybrid films with 25- and 65-nm SiO_2 as some silica particles were extracted from the matrix, indicating that there is incompatibility between large spherical particles and polymer matrix (phase separation). The TEM images of these hybrids are shown in Figure 4, and the results are in well accordance with that of SEM. The original SiO_2 particles aggregated to form large silica spheres with the size up to 2 μm. Especially, for the hybrid sample with 10-nm SiO_2 particles, we can clearly observe that the primary silica particles formed loose aggregation of spheres, while the close microspheres were formed in the hybrid samples with the large silica particles.

It is known that there are many silanol groups on the surface of silica particles without sintering at high temperature or modifying using organic molecules. Because of the small-size effect of nanoparticles, the small silica particles with large surface area have more silanol groups on surface of particles than that of large particles. So there is better interfacial interaction in hybrid film with 10-nm silica particles based on the strong interaction with carbonyl groups of polyimide chains through hydrogen bonding.[21,22] This result favors the improvement of properties of hybrids.

We also characterized the hybrid films using WAXD, and the X-ray patterns are shown in Figure 5. It can be seen that the hybrid films are amorphous structure. The effect of the content [Fig. 5(a)] and size [Fig. 5(b)] of SiO_2 on the morphology structures for polyimide has no obvious difference.

Thermal properties

The thermal properties of the hybrid films were studied by TGA, and the 5 wt % decomposition temperatures (T_d) of hybrid films are listed in Table II (PI/10-nm SiO_2 with different contents), Table III (PI/5 wt % SiO_2 with different SiO_2 sizes), and Table IV (PI/10 wt % SiO_2 with different SiO_2 sizes). It should be noted that the properties of hybrid films in Table II have large difference compared with Tables III and IV because these hybrid films were not prepared at one time. From Table II, it can be seen that the thermal stability of hybrid films decreases with increasing SiO_2 content. While the hybrid films with different sizes of SiO_2 exhibit an increasing trend for stability with increasing size of SiO_2, although their stability is lower than that of pure polyimide matrix (Tables III and IV). It maybe that the colloidal SiO_2 with small size has more uncondensed groups than large SiO_2, which results in the obvious decrease of the stability for hybrids with small size of SiO_2. On the whole, all the hybrid films exhibit good thermal stability ($T_d > 500$°C).

The T_g of the hybrid films were determined by DMTA, and the results are listed in Tables II–IV. The DMTA curves are also shown in Figures 6 and 7. It can be seen that as the 10-nm SiO_2 was incorpo-

TABLE III
Properties of PI/SiO_2 (5 wt %) Hybrid Films with Different Silica Particle Sizes

Samples	Modulus (MPa)	Tensile strength (MPa)	Elongation (%)	T_g (°C)	T_d (°C)
PI	1,430	130	55	382.7	572
PI-SiO_2 (10 nm)	1,660	166	54	399.4	549
PI-SiO_2 (25 nm)	1,540	148	52	392.8	560
PI-SiO_2 (65 nm)	1,450	115	45	388.1	569

TABLE IV
Properties of PI/SiO_2 (10 wt %) Hybrid Films with Different Silica Particle Sizes

Samples	Modulus (MPa)	Tensile strength (MPa)	Elongation (%)	T_g (°C)	T_d (°C)
PI	1,430	130	55	382.7	572
PI-SiO_2 (10 nm)	1,990	179	50	400.0	555
PI-SiO_2 (25 nm)	1,820	157	27	385.9	562
PI-SiO_2 (65 nm)	1,660	122	20	384.3	565

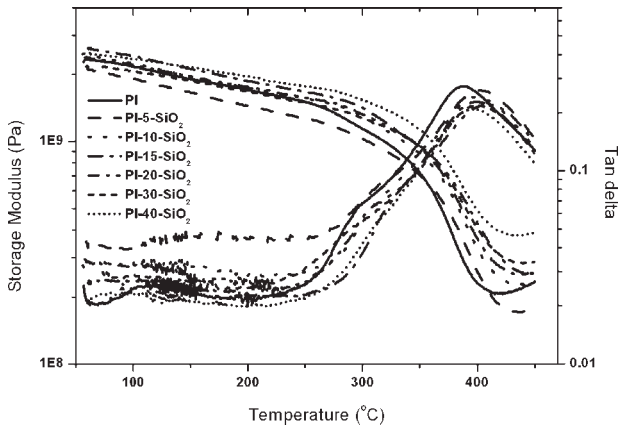

Figure 6 DMTA curves of PI/10-nm SiO_2 hybrid films with different SiO_2 contents.

rated into PI matrix, the T_g of PI in hybrid films increases by about 10°C in comparison with pure PI matrix, and this trend is less dependent on the content of SiO_2 (Table II). However, the T_g of hybrid films decreases with increasing SiO_2 size and these values are higher than that of pure PI. The hybrid films with different SiO_2 sizes for both 5 and 10 wt % SiO_2 exhibit the same trend (Tables III and IV). If we take no account of dispersion and aggregation state of SiO_2 particles in hybrid films, the above result indicates that the smaller size of SiO_2 has high surface area than that of large particles, and these small SiO_2 particles have stronger interaction with PI matrix and further restrict the segmental motion of polymers. SEM analyses also supported this result (Fig. 3). This phenomenon was also observed in other hybrid systems.[21,22]

Mechanical properties

The mechanical properties of the hybrid films were examined and the results are listed in Tables II–IV, respectively. For the PI/10-nm SiO_2 hybrid films with different SiO_2 contents, it can be seen from Table II that the modulus of hybrid films increases with increasing SiO_2 content, while the tensile strength and elongation at break decreases compared with the pure PI films. The dependence of mechanical properties of PI/SiO_2 on SiO_2 content was observed in other hybrid systems.[9,23–25] The effect of the colloidal SiO_2 size on the mechanical properties of hybrid films was also studied. It can be seen from Tables III and IV, when the content of SiO_2 is fixed (5 or 10 wt %) and SiO_2 particles with different sizes were introduced into PI matrix, there is a maximum value for hybrid films with 10-nm SiO_2 for the modulus and tensile strength, while hybrid films remain the higher elongation at break. In above discussion, the T_g of hybrid films also has the same trend. These results can be attributed to the better interfacial interaction between PI and the smaller SiO_2 particles as well as the development of the fine morphology in hybrid films, although there is larger aggregation in hybrid films. In addition, when the size of SiO_2 particles is fixed, the modulus and tensile strength of the nanocomposites increase from 5 to 10 wt % SiO_2, while the elongation at break decreases, especially for nanocomposites with large size of SiO_2. These results are in accordance with that in Table II, except the elongation at break.

Other properties

The densities and water absorption of the PI/10-nm SiO_2 hybrid films with different contents of SiO_2 were measured and the results are listed in Table II. The densities of the hybrid films gradually increase from 1.353 g/cm^3 for PI to 1.543 g/cm^3 for hybrid film with 40 wt % SiO_2, indicating that the SiO_2 particles (2.2 g/cm^3) have higher density than PI (1.35 g/cm^3). The water uptake of the hybrid films is

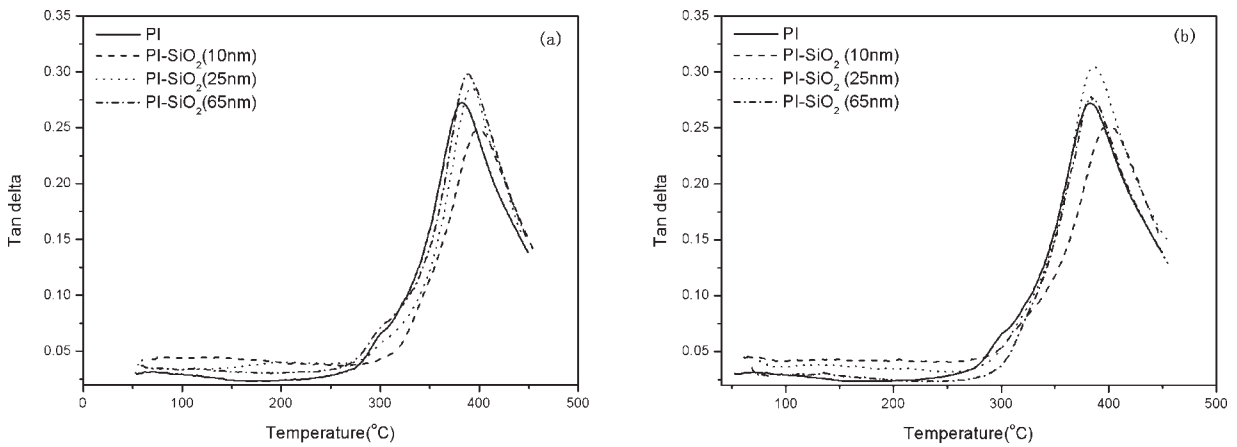

Figure 7 DMTA curves (tan δ) of PI/SiO_2 hybrid films with different sizes of SiO_2 and contents of (a) 5 wt % and (b) 10 wt %.

about 3.1–6.3 wt % and their values increase with increasing SiO_2 loading. This result indicates that the SiO_2 particle has a higher hydrophilicity than PI matrix because of the existence of hydroxyl groups at the surfaces of silica particles.

CONCLUSIONS

Different contents and sizes of SiO_2 were introduced into PI matrix by blending PAA and silica nanoparticles, followed by a step thermal imidization process. It was found that the modulus of hybrid films increased, while the tensile strength and elongation at break decreased with increasing SiO_2 content. When different sizes of SiO_2 particles were introduced into PI matrix, the hybrid films with small size of SiO_2 exhibited higher T_g and mechanical properties compared with other hybrid systems. In addition, all the hybrid films were amorphous and possessed good thermal stability ($T_d > 500^\circ C$). It was also expected that the microstructure and properties of hybrid films can be further improved by modifying the silica particles using surface decorating agents.

References

1. Caseri, W. Macromol Rapid Commun 2000, 21, 705.
2. Sanchez, C.; Ribot, F.; Lebeau, B. J Mater Chem 1999, 9, 35.
3. Sanchez, C.; Julián, B.; Belleville, P.; Popall, M. J Mater Chem 2005, 15, 3559.
4. Ding, M. X.; He, T. B. New Materials of Polyimide; Chinese Science Press: Beijing, 1998.
5. Ahmad, Z.; Mark, J. E. Chem Mater 2001, 13, 3320.
6. Chiang, P. C.; Whang, W. T. Polymer 2003, 44, 2249.
7. Kong, Y.; Du, H.; Yang, J.; Shi, D.; Wang, Y.; Zhang, Y.; Xin, W. Desalination 2002, 146, 49.
8. Beecroft, L. L.; Johnen, N. A.; Ober, C. K. Polym Adv Technol 1997, 8, 289.
9. Van Zyl, W. E.; García, M.; Schrauwen, B. A. G.; Kooi, B. J.; De Hosson, J. T. M.; Verweij, H. Macromol Mater Eng 2002, 287, 106.
10. Mustoa, P.; Ragostaa, G.; Scarinzia, G.; Masciab, L. Polymer 2004, 45, 4265.
11. Hsu, S. C.; Whang, W. T.; Hung, C. H.; Chiang, P. C.; Hsiao, Y. N. Macromol Chem Phys 2005, 206, 291.
12. Hide, F.; Nito, K.; Yasuda, A. Thin Solid Films 1994, 240, 157.
13. Lin, B.; Liu, H.; Zhang, S.; Yuan, C. J Solid State Chem 2004, 177, 3849.
14. Hedrick, J. L.; Cha, H. J.; Miller, R. D.; Yoon, D. Y.; Brown, H. R.; Srinivasan, S.; Di Pietro, R. Macromolecules 1997, 30, 8512.
15. Tamaki, R.; Choi, J.; Laine, R. M. Chem Mater 2003, 15, 793.
16. Huang, J. C.; He, C. B.; Xiao, Y.; Mya, K. Y.; Dai, J.; Siow, Y. P. Polymer 2003, 44, 4491.
17. Stöber, W.; Fink, A. J Colloid Interface Sci 1968, 26, 62.
18. Lü, C.; Wang, Z.; Liu, F.; Yan, J.; Gao, L. J Appl Polym Sci 2006, 100, 124.
19. Qiu, W.; Luo, Y.; Chen, F.; Duo, Y.; Tan, H. Polymer 2003, 44, 5821.
20. Musto, P.; Ragosta, G.; Scarinzi, G.; Mascia, L. Polymer 2004, 45, 1697.
21. Chen, Y.; Zhou, S.; Yang, H.; Wu, L. J Appl Polym Sci 2005, 95, 1032.
22. Li, F.; Zhou, S.; Wu, L. J Appl Polym Sci 2005, 98, 2274.
23. Zhu, Z. K.; Yang, Y.; Yin, J.; Qi, Z. N. J Appl Polym Sci 1999, 73, 2977.
24. Im, J. S.; Lee, J. H.; An, S. K.; Song, K. W.; Jo, N. J.; Lee, J. O.; Yoshinaga, K. J Appl Polym Sci 2006, 100, 2053.
25. Park, H. B.; Kim, J. H.; Kim, J. K.; Lee, Y. M. Macromol Rapid Commun 2002, 23, 544.